Combined Mössbauer and EPR Studies of the $S = 3$ State of an Exchange-Coupled $Fe^{III}Cu^{II}$ Complex: Test for Quantitative EPR Analysis of Integer Spin Systems

C. Juarez-Garcia,[†] M. P. Hendrich,[†] T. R. Holman,[‡] L. Que,[‡] and E. Münck*[,†,§]

Contribution from the Gray Freshwater Biological Institute, University of Minnesota, Navarre, Minnesota 55392, and the Department of Chemistry, University of Minnesota, Minneapolis, Minnesota 55455. *Received May 14, 1990*

Abstract: We have studied acetonitrile solutions of the bimetallic complex $[Fe^{III}Cu^{II}(BPMP)Cl_2](BPh_4)_2$, where BPMP is the anion 2,6-bis[(bis(2-pyridylmethyl)amino)methyl]-4-methylphenol, with Mössbauer and EPR spectroscopy. Both spectroscopic techniques show that the complex is ferromagnetically coupled ($\hat{H} = J\mathbf{S}_1\cdot\mathbf{S}_2$, $J < 0$) to yield a ground state spin $S = 3$. Analysis of the Mössbauer spectra taken in applied fields up to 6.0 T yielded for the Fe^{III} site the zero-field splitting parameters $D_1 = +1.2$ cm^{-1} and $E_1 = 0.11$ cm^{-1}, the magnetic hyperfine coupling constant $A_0 = -28.8$ MHz, quadrupole spitting $\Delta E_Q = 0.67$ mm/s, and isomer shift $\delta = 0.48$ mm/s. The zero-field splitting term of the ferric ion mixes the excited $S = 2$ multiplet with the ground manifold, the mixing being proportional to D_1/J; by analyzing this mixing we have determined that -2 cm$^{-1} > J > -5$ cm^{-1}. The $Fe^{III}Cu^{II}$ complex gives an X-band resonance at $g = 12$ which we have studied with a bimodal cavity in the temperature range from 2 to 50 K. We have analyzed the position and line shape of the $g = 12$ signal with a computer program in the framework of an $S = 3$ spin Hamiltonian, allowing a Gaussian distribution of the zero-field splitting parameters D and E. Finally, we have determined the $S = 3$ spin concentration from spectral simulations relative to a known standard; the value obtained agrees with the optically determined concentration. Our result shows that it is possible to determine spin concentrations of integer spin complexes with a precision that approaches that obtained for systems with half-integral spin. The availability of such techniques is highly desirable for the study of an ever increasing number of metalloproteins. We describe a method that allows one to determine the spin of the coupled system directly from the Mössbauer spectrum. Using this method we show here that the ground manifolds of $[Fe^{III}Cu^{II}(BPMP)Cl_2](BPh_4)_2$ and $[Fe^{III}Cu^{II}BPMP(OAc)_2](BPh_4)_2$ have $S = 3$ and 2, respectively. At $T = 93$ K the zero-field Mössbauer spectrum of the integer spin complex $[Fe^{III}Cu^{II}(BPMP)Cl_2](BPh_4)_2$ exhibits unusual line broadening, similar to that observed for *Thermus thermophilus* cytochrome c_1aa_3.

Introduction

For a few years our groups have been studying the electronic structure of the diferrous states of the binuclear clusters of iron–oxo proteins. Using Mössbauer and EPR spectroscopy as well as SQUID magnetometry we have investigated the clusters of methane monooxygenase[1] and ribonucleotide reductase[2] and the synthetic complex $[Fe^{II}Fe^{II}BPMP(OPr)_2](BPh_4)$.[3] We have not yet succeeded in analyzing the data sets with a unified model, primarily because of the staggering complexities of the multiparameter problems. Thus, in the framework of a spin Hamiltonian a description of the low-lying electronic levels requires two zero-field splitting tensors, $\mathbf{D}_1$ and $\mathbf{D}_2$, two $\mathbf{g}$ tensors, and a parameter, J, describing the exchange interaction. According to our current understanding of the above-mentioned complexes, the magnitude of the exchange coupling is comparable to that of the zero-field splittings. For such systems, the total spin S is not a good quantum number. Quite interestingly, all of the clusters studied exhibit EPR spectra with intense resonances at low magnetic field, thus adding another spectroscopic tool for the investigation of these integer spin systems.

Aside from the above-mentioned compounds, EPR has been applied in the studies of other integer spin systems having biological relevance, for example, cytochrome c oxidase[4] and the azide complex of deoxyhemerythrin.[5] Typically, there has not been a quantitative treatment of signal intensities, but such treatment is quite useful for two reasons. First, it provides a check of the assignment of the resonance to the correct spin doublet, and second, it allows for the determination of the concentration of the complex. Because this treatment has only recently been applied for the study of such systems,[1,6] we lack experience in interpreting the observed spectra both qualitatively and quantitatively. Mössbauer spectroscopy, which is sensitive to J, $\mathbf{D}_1$, and $\mathbf{D}_2$, and to a lesser degree to the $\mathbf{g}$ tensors, thus far has not yielded decisive clues for the determination of the electronic parameters, not for a lack of sensitivity but because the spectra depend additionally on two magnetic hyperfine tensors and two electric field gradient tensors, all of which may have different principal axis frames. In order to study the fundamental features of EPR and Mössbauer spectroscopy of exchange-coupled, non-Kramers systems in detail, we have chosen a complex with two desirable properties. First, the complex exhibits EPR signals typical of those observed of exchange-coupled binuclear centers. Second, the complex contains a high-spin ferric ion ($S_1 = {}^5/_2$) exchange coupled to a metal with $S_2 = {}^1/_2$. Since the magnetic hyperfine interaction of high-spin Fe^{III} is isotropic and the quadrupole interactions are small, the ^{57}Fe hyperfine parameters are readily determined. With the hyperfine parameters known, the high precision of Mössbauer spectroscopy can be used to determine $\mathbf{D}_1$ and the percentage of total iron belonging to the EPR active species, and thus it provides crucial information for cross-checking the interpretation of the EPR data.

In this paper we report the Mössbauer and EPR spectra of the integer spin complex $[Fe^{III}Cu^{II}(BPMP)Cl_2](BPh_4)_2$. The Mössbauer spectra as well as the EPR data were analyzed quantitatively with spectral simulations using a spin Hamiltonian of an exchange-coupled pair. The successful simulations of the EPR spectra allowed us to determine the spin concentration of the complex. The cluster concentration obtained by EPR agrees well with that determined optically. The results reported here, together with recent work on similar EPR signals,[6] show that the

[†] Gray Freshwater Biological Institute.
[‡] Department of Chemistry.
[§] New address: Department of Chemistry, Carnegie Mellon University, Pittsburgh, PA 15213.

(1) Hendrich, M. P.; Münck, E.; Fox, B. G.; Lipscomb, J. D. *J. Am. Chem. Soc.* **1990**, *112*, 5861–5865.
(2) Lynch, J. B.; Juarez-Garcia, C.; Münck, E.; Que, L., Jr. *J. Biol. Chem.* **1989**, *264*, 8091–8096.
(3) Borovik, A. S.; Hendrich, M. P.; Holman, T. R.; Münck, E.; Papaefthymiou, V.; Que, L., Jr. *J. Am. Chem. Soc.* **1990**, *112*, 6031–6038.
(4) (a) Dunham, W. R.; Sands, R. H.; Shaw, R. W.; Beinert, H. *Biochim. Biophys. Acta* **1983**, *748*, 73–85. (b) Hagen, W. R.; Dunham, W. R.; Sands, R. H.; Shaw, R. W.; Beinert, H. *Biochim. Biophys. Acta* **1984**, *765*, 399–402. (c) Hagen, W. R. *Biochim. Biophys. Acta* **1982**, *708*, 82–98. (d) Brudvig, G. W.; Morse, R. H.; Chan, S. I. *J. Magn. Reson.* **1986**, *67*, 189–201.
(5) (a) Reem, R. C.; Solomon, E. I. *J. Am. Chem. Soc.* **1984**, *106*, 8323–8325. (b) Reem, R. C.; Solomon, E. I. *J. Am. Chem. Soc.* **1987**, *109*, 1216–1226.
(6) Hendrich, M. P.; Debrunner, P. G. *Biophys. J.* **1989**, *56*, 489–506.

0002-7863/91/1513-518$02.50/0

spin concentration of non-Kramers systems can be determined with a precision that approaches those obtained for Kramers systems.

Experimental Section

All reagents and solvents were purchased from commercial sources and used as received, unless noted otherwise. Microanalyses were performed by Desert Analytics, Inc., Tucson, AZ. The ligand 2,6-bis-[(bis(2-pyridylmethyl)amino)methyl]methylphenol (HBPMP) was synthesized by published methods.[7]

Dichloro(2,6-bis[(bis(2-pyridylmethyl)amino)methyl]-4-methylphenolato)iron(III)copper(II) Bis(tetraphenylborate), $[Fe^{III}Cu^{II}(BPMP)Cl_2](BPh_4)_2$. A solution of 0.040 g (0.076 mmol) of HBPMP in 10 mL of methanol was treated with a solution of 0.021 g (0.076 mmol) of $FeCl_3 \cdot 6H_2O$ in 5 mL of methanol to yield a dark blue solution, which contains the mononuclear iron complex. Sequential addition of 0.013 g (0.076 mmol) of $CuCl_2 \cdot 2H_2O$ in 5 mL of methanol and a methanolic solution of sodium tetraphenylborate (0.104 g, 0.304 mmol) afforded a green solid, which was filtered and dried. Further purification was achieved by recrystallization of the crude product by vapor diffusion of methanol into an acetone solution of complex. Anal. Calcd for $C_{81}H_{73}B_2Cl_2CuFeN_6O_1$: C, 71.62; H, 5.42; Cl, 5.22; Cu, 4.68; Fe, 4.11; N, 6.19. Found: C, 71.79; H, 5.58; Cl, 4.98; Cu, 4.46; Fe, 3.93; N, 6.11. UV-vis (acetonitrile): λ_{max} 385 nm (sh), 604 nm (ϵ = 1400 M^{-1} cm^{-1}).

The ^{57}Fe sample was synthesized from 70% enriched $^{57}Fe_2O_3$ dissolved in concentrated HCl. The $^{57}FeCl_3$ salt was isolated and the procedure described above was then employed to yield suitable crystals.

Bis(μ-acetato-*O*,*O'*)(2,6-bis[(bis(2-pyridylmethyl)amino)methyl]-4-methylphenolato)iron(III)copper(II) Bis(tetraphenylborate), $[Fe^{III}Cu^{II}BPMP(OAc)_2](BPh_4)_2$. Treatment of an acetone solution of the $[Fe^{III}Cu^{II}(BPMP)Cl_2](BPh_4)_2$ complex with 2.2 equiv of AgOAc afforded a purplish brown solution which was filtered to remove the AgCl solid. Vapor diffusion of ethyl acetate into the acetone solution gave rise to crystals, $[Fe^{III}Cu^{II}BPMP(OAc)_2](BPh_4)_2$ (50% yield). Anal. Calcd for $C_{85}H_{79}B_2CuFeN_6O_5$: C, 72.63; H, 5.66; N, 5.98; Cu, 4.52; Fe, 3.97. Found: C, 73.06; H, 5.73; N, 6.00; Cu, 4.69; Fe, 4.02. UV-vis (CH_3COCH_3): λ_{sh} = 500 nm.

X-band EPR spectra were recorded on a Varian E9 spectrometer with an Oxford liquid helium flow cryostat and a Varian Model E-236 bimodal cavity. The magnetic field was calibrated with an NMR gaussmeter. Computer simulations were generated by diagonalization of the spin Hamiltonian of eq 2. The simulation program was formulated in accordance with eq 12 of ref 6 with modifications appropriate for a spin $S = 3$ spin Hamiltonian. For comments pertaining to the program see refs 1 and 6. Due to the use of an additional distribution in the zero-field parameter D, the calculations required approximately 5 min of processor time on a CDC Cyber 175 computer.

Iron-doped zinc fluorosilicate crystals were prepared as described previously.[6] The percentage of iron in the crystals was 1.49 ± 0.03 as measured by plasma emission spectroscopy.

Results and Discussion

The high affinity of phenolate for Fe^{III} allows the formation of the monoiron complex of the binucleating ligand BPMP without contamination from the diiron derivative. This large difference in the ferric ion affinities has led to the synthesis of heterobimetallic complexes containing Fe^{III}, i.e. $Fe^{III}M^{II}BPMP$.[7c,d,8] $[Fe^{III}Cu^{II}(BPMP)Cl_2](BPh_4)_2$ has been obtained by sequential addition of $FeCl_3$ and $CuCl_2$ to a BPMP solution, followed by metathesis with $NaBPh_4$. X-ray diffraction studies[9] on crystals obtained from acetone/methanol reveal a binuclear complex with the iron and the copper atoms bridged solely by the phenolate oxygen of BPMP (Figure 1). The Cu^{II} site is square pyramidal with the phenolate oxygen at the apex and three nitrogen atoms of BPMP and terminal chloride constituting the base. The Fe^{III} site has an octahedral coordination environment with an additional methanol ligand (presumably derived from the recrystallization solvent)

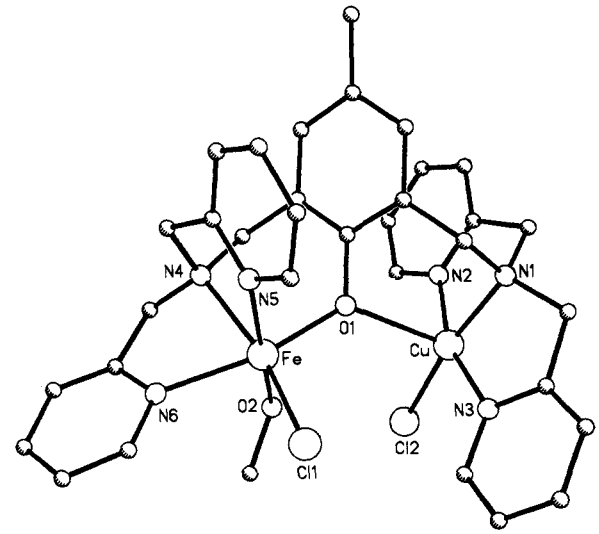

Figure 1. Structure of the dinuclear cation[9] $[Fe^{III}Cu^{II}(BPMP)Cl_2HOMe]^{2+}$.

occupying one of the coordination sites. The methanol ligand appears to be readily lost, as polycrystalline material which had been dried in vacuo afforded elemental analyses consistent with the absence of the methanol.

We have studied the Mössbauer and EPR spectra of $[Fe^{III}Cu^{II}(BPMP)Cl_2](BPh_4)_2$ as a polycrystalline solid and in a variety of solvents; the spectra differ between solid and solution and were somewhat solvent dependent. The observed variations can be readily rationalized by the lability of the ligand trans to the phenolate oxygen on the iron; this position is unoccupied in the polycrystalline solid and presumably occupied by a solvent molecule in the various solutions. In this paper we describe the properties of the complex in acetonitrile (called complex **1**) focussing on the relationships between the Mössbauer and EPR results.

Spin Hamiltonian for Analyses of Mössbauer and EPR Spectra. The complex to be described consists of an exchange-coupled pair of Fe^{III} ($S_1 = {}^5/_2$) and Cu^{II} ($S_2 = {}^1/_2$) ions. The spin Hamiltonian which describes the magnetic properties of the low-lying electronic state is

$$\hat{H} = J\mathbf{S}_1\cdot\mathbf{S}_2 + D_1[S_{1z}^2 - 35/12 + (E_1/D_1)(S_{1x}^2 - S_{1y}^2)] + g_1\beta\mathbf{S}_1\cdot\mathbf{H} + \beta\mathbf{S}_2\cdot\mathbf{g}_2\cdot\mathbf{H} \quad (1)$$

where J is the exchange-coupling parameter, D_1 and E_1 are the zero-field splitting parameters of the ferric ion, and the last two terms describe the Zeeman interactions. As shown below, for the complex treated here we have $J \approx -3$ cm^{-1}, $D_1 \approx 1.2$ cm^{-1}, $\mathbf{g}_1 = 2.0$, and $\mathbf{g}_2 = 2.0 + \Delta\mathbf{g}_2$, where the components of $\Delta\mathbf{g}_2$ are expected to be small. For $|J| \geq 3$ cm^{-1}, the low-lying energy levels divide into two multiplets with $S = 3$ and 2, separated by $3J$ in energy. Under these conditions, it is useful to discuss the problem in a coupled representation, replacing $\mathbf{S}_1$ and $\mathbf{S}_2$ by the system spin, $\mathbf{S} = \mathbf{S}_1 + \mathbf{S}_2$. The electronic properties of the $S = 3$ multiplet can then be described by

$$\hat{H}_e = D[S_z^2 - 4 + (E/D)(S_x^2 - S_y^2)] + \beta\mathbf{S}\cdot\mathbf{g}\cdot\mathbf{H} \quad (2)$$

where the quantities D, E/D, and $\mathbf{g}$ refer now to the coupled system. Application of the Wigner–Eckart theorem yields for the $S = 3$ multiplet[10]

$$\mathbf{D} = (2/3)\mathbf{D}_1 \quad (3)$$

and

$$\mathbf{g} = (5/6)\mathbf{g}_1 + (1/6)\mathbf{g}_2 \quad (4)$$

These expressions are correct for $|J| \gg |D_1|$. If the magnitudes of J and D_1 are comparable, the zero-field splitting term of eq 1 can mix the $S = 3$ and 2 multiplets; although this mixing is quite

(7) (a) Suzuki, M.; Kanatomi, H.; Murase, I. *Chem. Lett., Chem. Soc. Jpn.* **1981**, 1745–1748. (b) Borovik, A. S.; Papaefthymiou, V.; Taylor, L. F.; Anderson, O. P.; Que, L., Jr. *J. Am. Chem. Soc.* **1989**, *111*, 6183–6195. (c) Suzuki, M.; Uehara, A.; Oshio, H.; Endo, K.; Yanaga, M.; Kida, S.; Saito, K. *Bull. Chem. Soc. Jpn.* **1987**, *60*, 3547–3555. (d) Borovik, A. S.; Que, L., Jr.; Papaefthymiou, V.; Münck, E.; Taylor, L. F.; Anderson, O. P. *J. Am. Chem. Soc.* **1988**, *110*, 1986–1988.

(8) Holman, T. R.; Juarez-Garcia, C.; Hendrich, M. P.; Que, L., Jr.; Münck, E. *J. Am. Chem. Soc.* **1990**, *112*, 7611–7618.

(9) Andersen, K.; Anderson, O. P. Unpublished results. Details of the crystallographic analysis will be published elsewhere.

(10) Scaringe, R. P.; Hodgson, D. K.; Hatfield, W. E. *Mol. Phys.* **1978**, *35*, 701–713.

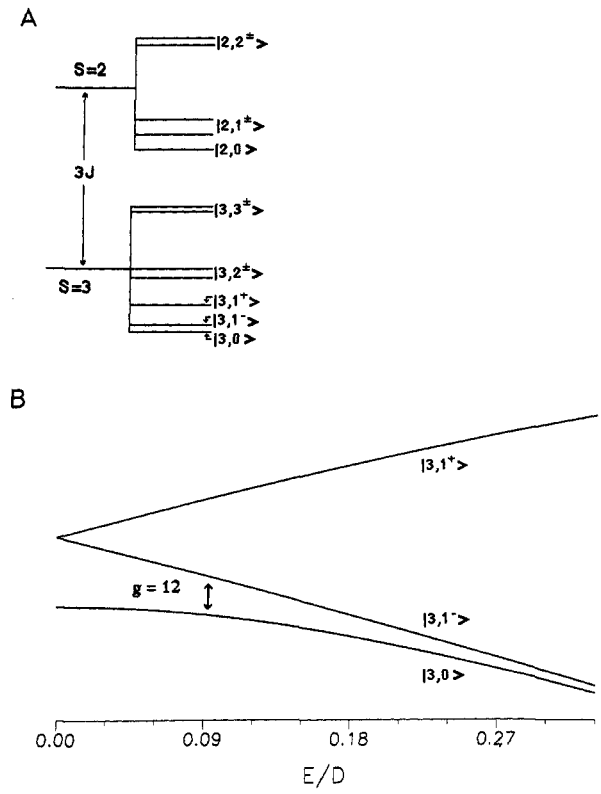

Figure 2. Energy level diagram of $[Fe^{III}Cu^{II}(BPMP)Cl_2](BPh_4)_2$ according to eq 1 for $J < 0$, $D_1 > 0$, $(E_1/D_1) = 0.09$, and $H = 0$ (A). Part B shows the energies of the three lowest states as a function of $E/D = E_1/D_1$.

small for the compound described here, it is measurable by Mössbauer spectroscopy. For the experimental conditions employed, multiplet mixing due to the anisotropy of $\mathbf{g}_2$ can be ignored. Figure 2A shows an energy level diagram obtained from eq 1 for $H = 0$.

Equation 2 is sufficient for analyzing the EPR data. For the analysis of the Mössbauer spectra it needs to be amended by terms describing the hyperfine interactions of the ^{57}Fe

$$\hat{H}_{hf} = A\mathbf{S}\cdot\mathbf{I} + \frac{eQV_{zz}}{12}[3I_z^2 - 15/4 + \eta(I_x^2 - I_y^2)] - g_n\beta_n\mathbf{H}\cdot\mathbf{I} \quad (5)$$

where all quantities have their conventional meanings. The A value in the coupled representation is related to the intrinsic A value of the ferric site by $A = (5/6)A_1$. The Mössbauer spectra can be computed by diagonalization of

$$\hat{H}_T = \hat{H}_e + \hat{H}_{hf} \quad (6)$$

It will be useful to discuss here briefly an interesting feature of the Mössbauer spectra recorded in strong applied fields. The magnetic splittings of the Mössbauer spectra reflect an effective field acting on the nucleus, $\mathbf{H}_{eff} = \mathbf{H}_{int} + \mathbf{H}$, where the internal field, $\mathbf{H}_{int}$, is given by

$$\mathbf{H}_{int} = -\langle\mathbf{S}\rangle A/g_n\beta_n \quad (7)$$

Here we have made use of the fact that the magnetic hyperfine interaction of the high-spin Fe^{III} ion is isotropic. By measuring the internal field we obtain the expectation value of the electronic spin, $\langle\mathbf{S}\rangle$, which is determined by the parameters of eq 2. An interesting situation occurs when the electronic Zeeman splitting is large compared to the zero-field splitting. Choosing for convenience the direction of the applied field as the quantization axis, we obtain $H_{int} = -AM/g_n\beta_n$ where M is the magnetic quantum number. If the electronic spin relaxes slowly on the time scale of Mössbauer spectroscopy (≈10 MHz for the complex considered here), one can observe a distinct Mössbauer spectrum for each possible M value of a multiplet. For $\mathbf{g} = 2$ and $H = 5.0$ T, only

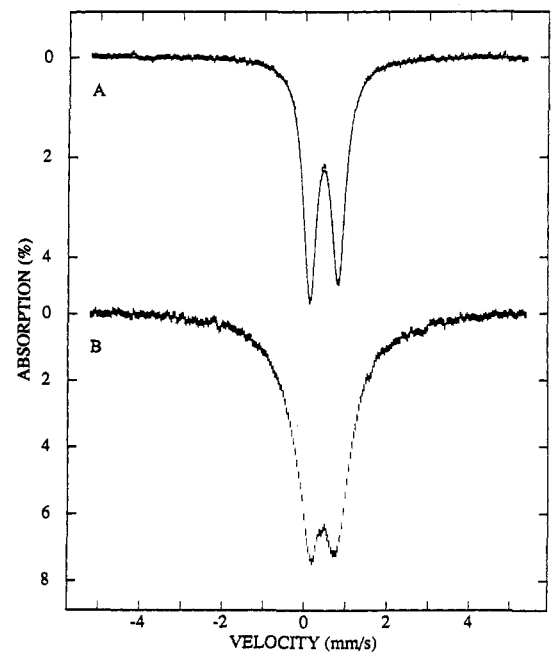

Figure 3. Mössbauer spectra of ^{57}Fe-enriched $[Fe^{III}Cu^{II}(BPMP)Cl_2](BPh_4)_2$ (~1.5 mM) in acetonitrile. The spectra were recorded in zero field at 1.5 (A) and 93 K (B). In order to shield the sample from the fringe magnetic field of the transducer, the sample chamber was surrounded by a sheet of μ-metal to give $B < 10^{-4}$ T at the sample.

the states with $M = -S$ (≈84%) and $M = -(S-1)$ are appreciably populated at $T = 4.2$ K. It follows from eq 7 that the ratio of the internal fields of the associated Mössbauer spectra is $(S-1)/S$. This ratio is 2/3 and 1/2 for the $S = 3$ and 2 multiplets, respectively. By measuring the ratio of the internal fields, the value of S for the ground multiplet is readily determined from the Mössbauer spectrum (see Figures 4 and 6).

Mössbauer Studies of $[Fe^{III}Cu^{II}(BPMP)Cl_2](BPh_4)_2$ in Acetonitrile. A 1.5 K Mössbauer spectrum of complex **1** dissolved in acetonitrile is shown in Figure 3A. The spectrum, recorded in zero field, consists of a doublet with $\Delta E_Q = 0.67$ (2) mm/s and $\delta = 0.48$ (1) mm/s. These parameters are characteristic of high-spin $(S_1 = {}^5/_2)$ Fe^{III}.

Figure 4 shows spectra of complex **1** recorded in a parallel applied field of 5.0 T. The 1.5 K spectrum of Figure 4A is typical of an isotropic system for which nuclear $\Delta m = 0$ transitions (arrows in Figure 4A) are essentially quenched. This observation shows that, for $H = 5.0$ T, the electronic Zeeman term dominates the zero-field splitting. The 4.2 K spectrum of Figure 4B exhibits a noticeably increased absorption at velocities slightly larger than those at which the $\Delta m = 0$ transitions appear (arrows in Figure 4B). This additional absorption is attributable to the population of a low-lying excited state. By subtracting 84% of the area of the spectrum of Figure 4A from that of Figure 4B we obtained the spectrum of Figure 4C which represents the first excited state. The ratio of the magnetic splittings of spectra C and A of Figure 4 is $R = 0.64$ from which we conclude, using the arguments given above, that the ground-state manifold has $S = 3$. Thus, the $Fe^{III}Cu^{II}$ complex is ferromagnetically coupled.

We have studied complex **1** at 4.2 and 1.5 K in applied fields of 0.5, 1.0, 3.0, 5.0, and 6.0 T. The spectra were analyzed by means of spectral simultations based on eq 6. For the analysis we used extensively a variety of graphics routines which plotted $\langle\mathbf{S}_{1i}\rangle$ and $\langle\mathbf{S}_i\rangle$ for eqs 1 and 2, $i = x, y, z$.

Before we collected the Mössbauer spectra of complex **1** we had struggled with the analysis of the EPR spectra. We initially attempted to associate the $g = 12$ resonance (see below) with $\Delta M_S = 0$ transitions between the members of the ground doublet of an $S = 3$ multiplet with $D < 0$. By using a nomenclature appropriate to the EPR conditions ($\beta H \ll D$) this doublet can be designated with $|3,3^{\pm}\rangle = (|3,M_S = +3\rangle \pm |3,M_S = -3\rangle)/\sqrt{2}$ where $|M_S\rangle$ refers to the z axis of the zero-field splitting tensor.[11]

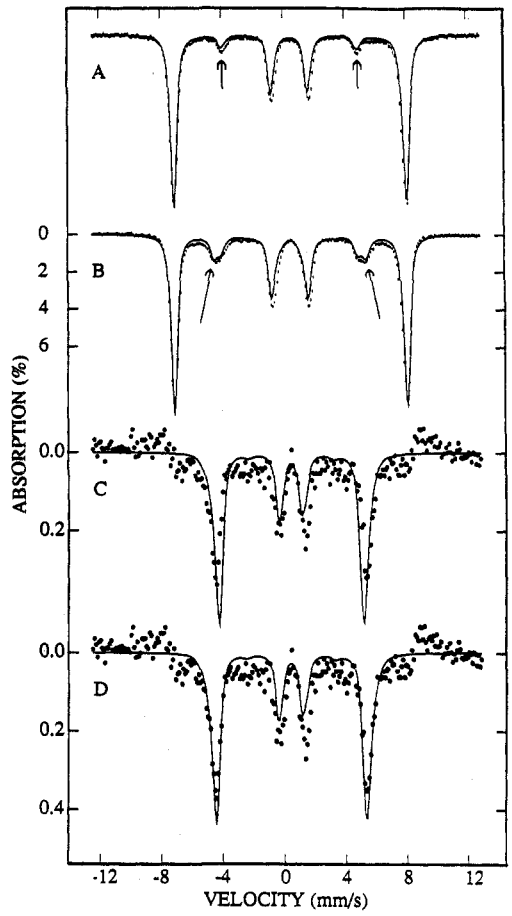

Figure 4. Mössbauer spectra of $[Fe^{III}Cu^{II}(BPMP)Cl_2](BPh_4)_2$ dissolved in acetonitrile. Spectra were recorded at 1.5 (A) and 4.2 K (B) in a parallel applied field of 5.0 T. The "experimental" spectra in C and D were obtained by subtracting the 1.5 K spectrum A from that of spectrum B, assuming that 84% of the area of spectrum B results from the electronic ground state $M_S = -3$. The difference spectrum can be attributed to the first excited state with $S = 3$ and $M_S = -2$. The solid lines in spectra A, B, and D are spectral simulations using the parameters listed in Table I. The theoretical spectrum C was computed with the same parameter set, except that $|J| \gg D_1$. The arrows in A indicate the nuclear $\Delta m = 0$ transitions.

However, we noted that the splitting of this doublet in zero field was quite small and did not give satisfactory EPR simulations. Our attention became focussed on a different doublet when the high-field 1.5 K Mössbauer spectra became available. These spectra showed that the magnitude of $\mathbf{H}_{int}$, i.e. the magnitude of $\langle \mathbf{S}_i \rangle$, is 9% smaller in an applied field $H = 1.0$ T than in $H = 6.0$ T. In order to produce a 9% decrease for $\langle \mathbf{S}_i \rangle$ for the lowest level of an $S = 3$ multiplet for $D < 0$, the value for D must be unreasonably large, namely $|D| > 25$ cm^{-1}. This, of course, contradicts our finding that βH is larger than $|D|$ for $H = 5.0$ T. Thus, the Mössbauer spectra forced us to conclude that $D > 0$, and they directed us to assign the EPR resonance to a different ground doublet, namely to $\Delta M_S = \pm 1$ transitions between the $|3,0\rangle$ and $|3,1^-\rangle$ levels.

By fitting the field dependence of $\mathbf{H}_{int}$, we have determined the zero-field splitting parameters of eq 1, obtaining $D_1 = +1.2$ cm^{-1} and $E_1/D_1 = 0.09$, or equivalently $D = 0.8$ cm^{-1} and $E/D = 0.09$ if we use eq 2 for the description of the data. Quite interestingly, the small value of E_1/D_1 allowed us to obtain a good estimate for J from the 5.0 T Mössbauer spectra. The argument is as follows. The zero-field splitting term of eq 1 mixes the substates of the $S = 3$ multiplet with those of the $S = 2$ manifold. For small E_1/D_1 we need to consider only $D_1(S_{1z}^2 - 35/12)$. This term mixes states with the same M_S value.[10] Because the $S = 2$ multiplet lacks a state with $M_S = -3$, the electronic ground state, $|S = 3, M_S = -3\rangle$ is not affected by mixing. At $H = 5.0$ T, this state has $\langle S_z \rangle = M_S = -3.0$ quite independent of D_1 and J. Therefore, the magnetic hyperfine coupling constant, $A_1 = (6/5)A = -28.8$ MHz, is readily determined from the spectrum of Figure 4A. On the other hand, the first excited state, $|S = 3, M_S = -2\rangle$, can mix with the $|S = 2, M_S = -2\rangle$ level, the mixing being proportional to D_1/J. For the ratio of the magnetic splittings of the $|S = 3, M_S = -2\rangle$ and $|S = 3, M_S = -3\rangle$ levels one obtains $R = {}^2/_3$ in the limit $D_1 = 0$ and $R = 0.62$ for $D_1 = 1.2$ cm^{-1} and $|J| \gg D_1$; experimentally, we observed $R = 0.64$. As can be seen from inspection of Figure 4C, a simulation with $|J| \gg D_1$ yields an excited state spectrum with insufficient splitting. The splitting can be increased by lowering the magnitude of J. A good match for the experimental splittings was obtained for -2 cm$^{-1} > J > -5$ cm^{-1};[12] a fit for J

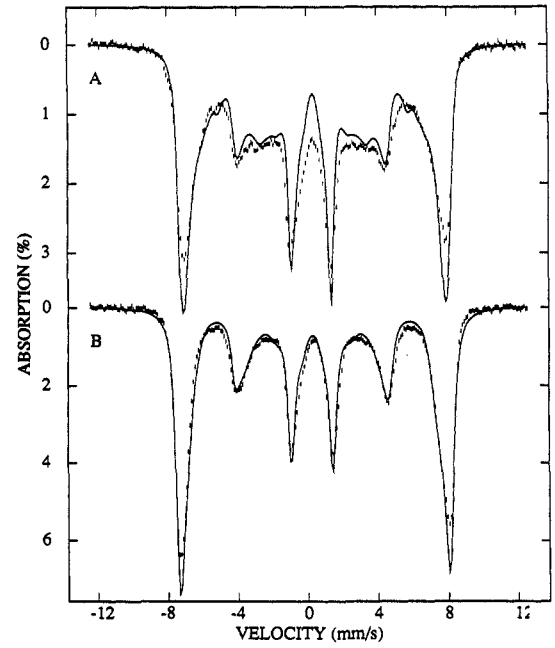

Figure 5. 1.5 K Mössbauer spectra of $[Fe^{III}Cu^{II}(BPMP)Cl_2](BPh_4)_2$ recorded in 0.5 (A) and 1.0 T (B) parallel applied fields. The solid line in part B is a spectral simulation using the parameters of Table I. The theoretical curve in part A was generated from the same parameter set, except that E_1/D_1 was assumed to have a Gaussian distribution of width $\sigma = 0.05$ centered at $E_1/D_1 = 0.09$.

Table I. Parameters Used To Simulate the Mössbauer Spectra of Figures 4 and 5[a]

D_1, cm^{-1}	+1.2 (1)	ΔE_Q, mm/s	0.67 (2)
E_1, cm^{-1}	0.11 (2)	η	−0.6
A_1, MHz	−28.8 (4)	δ, mm/s	0.48 (1)

[a] The spectra were fitted to eq 1 by using $J = -3$ cm^{-1} and $g_1 = g_2 = 2.0$. For the simulations we have tilted the z axis of the electronic field gradient tensor by $\beta = 45°$ relative to the z axis of the zero-field splitting tensor; however, the value of β is quite soft as we could not exclude the possibility that $\beta = 0°$. Numbers in parentheses give estimated uncertainties of the least significant digit.

(11) In discussing our results we are using different quantization axes for the EPR and Mössbauer data. The relevant EPR resonances are observed at fields below 0.1 T. Under these conditions the zero-field splitting dominates and the levels are best described in the frame of the D tensor, with the M quantum numbers referring to the z axis of this tensor. For the 5.0 T Mössbauer data the Zeeman term dominates and it is therefore more convenient, for discussing the spectra, to choose the quantization axis along the applied field. Since the splittings depend strongly on the direction of the applied field relative to the D tensor and since there are extensive level crossings at fields of intermediate strength, 1.0 T < H < 4.0 T, the situation is not conveniently described by a single graph.

(12) We have measured the magnetic susceptibility of polycrystalline $[Fe^{III}Cu^{II}(BPMP)Cl_2](BPh_4)_2$ and of an acetonitrile solution. The data of the solid compound are fitted well with $J = -3$ cm^{-1}. It appears that the J value of complex **1** is very similar to that of the solid; however, we have difficulties fitting the solution data to an acceptable accuracy, perhaps because we have not taken heterogeneities and minor copper impurities into account.

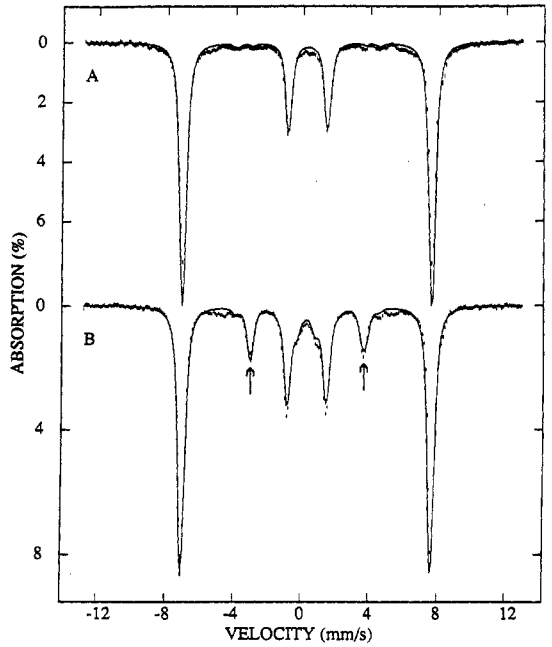

Figure 6. Mössbauer spectra of $[Fe^{III}Cu^{II}BPMP(OAc)_2](BPh_4)_2$ dissolved in acetonitrile. The spectra were recorded at 1.5 (A) and 4.2 K (B) in a parallel applied field of 5.0 T. The solid lines are theoretical curves fitted to a spin Hamiltonian with $S = 2$ using $A_1 = -29.7$ MHz, $\Delta E_Q = 0.42$ mm/s, $\delta = 0.46$ mm/s, $D = 0.5$ cm^{-1}, and $E/D = 0.33$. The spectra shown are meant to illustrate how the spin of the complex can be determined from high-field Mössbauer studies. The arrows in part B mark the outer lines of the Mössbauer spectrum of the first excited state, $|S = 2, M_S = -1\rangle$.

$= -3$ cm^{-1} is shown in Figure 4D.

The solid lines in Figures 4 and 5B are spectral simulations based on eq 6 with use of the parameter set of Table I. Fits of similar quality were obtained for data obtained for 3.0 or 6.0 T applied fields. For the 0.5 T spectrum of Figure 5A, the theory predicts the correct line positions but the simulations produce spectra with too narrow lines. We have learned recently from Mössbauer and EPR studies of related complexes that the low-field spectra exhibit strain, i.e. the zero-field splitting parameter E_1/D_1 is distributed.[8] The theoretical curve in Figure 5B was generated with the parameter set of Table I but allowing a distribution of E_1/D_1 over a Gaussian envelope with width $\sigma = 0.05$ around its mean $E_1/D_1 = 0.09$. Although the theoretical curve describes the data quite well, the theory still produces slightly too much intensity in the outer lines. Most likely this mismatch is attributable to relaxation effects. It appears that the electronic spin relaxation time is not long on the Mössbauer time scale for all molecular orientations; this is supported by the observation that a 1.0 T spectrum recorded at 4.2 T showed broadening of the outermost lines relative to the corresponding 1.4 K spectrum.

We have also recorded Mössbauer spectra of polycrystalline $[Fe^{III}Cu^{II}(BPMP)Cl_2](BPh_4)_2$. This material has $\Delta E_Q = 0.85$ (2) mm/s, $A_1 = -29.1$ (4) MHz, and $\delta = 0.46$ (2) mm/s and thus parameters that are similar to but distinct from complex **1**, supporting our suggestion that the vacant site of the polycrystalline material may be occupied by a solvent molecule in acetonitrile solution.

We have argued above that one can determine the spin of the complex directly from the 5.0 T Mössbauer spectra. For complex **1** we deduced that the ground manifold has $S = 3$ and that complex **1** is, therefore, ferromagnetically coupled. We are currently studying a related complex, namely $[Fe^{III}Cu^{II}BPMP(OAc)_2](BPh_4)_2$.[13] Figure 6 shows two 5.0 T Mössbauer spectra of this complex, measured at 1.5 (A) and 4.2 K (B), and their corresponding spectral simulations. In Figure 6 the outer lines of the spectrum of the first excited state are marked by arrows. The ratio of the hyperfine fields of the first excited state and the ground state is $R = (S - 1)/S = 0.5$, from which we infer that $S = 2$, i.e. the complex is antiferromagnetically coupled. This agrees well with preliminary susceptibility studies which yield $J \approx +50$ cm^{-1};[14] we will report the results of Mössbauer, EPR, and susceptibility studies elsewhere. A comparison of the spectra of Figures 3 and 6 shows that determination of the spin with Mössbauer spectroscopy is straightforward for the compounds studied here.

Finally, we wish to comment on the zero-field Mössbauer spectra of Figure 3. It can be seen that the 1.5 K spectrum consists of a quadrupole doublet with reasonably sharp lines (fwhm = 0.40 mm/s). Quite surprisingly, the spectrum recorded at 93 K exhibits considerable line broadening. It is quite unlikely that this broadening of the zero-field spectrum is caused by static magnetic hyperfine interactions because time-reversal symmetry requires that $\langle \mathbf{S} \rangle = 0$, and therefore $\mathbf{H}_{int} = 0$, for any nondegenerate state. Integer spin complexes with magnetically isolated centers can exhibit zero-field magnetic hyperfine interactions only if the energy separation of two electronic levels is comparable to the hyperfine energies. This requires that the two levels be separated by less than 10^{-3} cm^{-1}, a condition not fulfilled for either the $S = 3$ or 2 multiplet of complex **1**. The shape of the spectrum of Figure 3B reminds us very much of those observed for high-spin Fe^{III} compounds with intermediate relaxation rates of the electronic spin.[15] This suggests that the spectrum of Figure 3B reflects a partial decoupling of the exchange interactions by spin–lattice relaxation processes at the Fe^{III} or Cu^{II} site. (This would be somewhat analogous to spin-decoupling in NMR double-irradiation experiments, except that the process that flips the local spin here would be stochastic.) It is interesting to note that the more strongly coupled $[Fe^{III}Cu^{II}BPMP(OAc)_2](BPh_4)_2$ does not exhibit any broadening at 100 K (data not shown). Line broadening similar to that of complex **1** has been reported for cytochrome a_3 of cytochrome oxidase isolated from *Thermus thermophilus*.[16] For this oxidase, the cytochrome a_3 is spin coupled to a cupric ion, Cu_B. Analysis of the coupling for the oxidase gives a solution which allows a very small J value, namely $|J| \approx 1$ cm^{-1}.[17] Line broadening has also been reported by Sage et al. for the spin-coupled cluster of $Fe^{III}Fe^{II}$ purple acid phosphatase.[18] We have considered a variety of mechanisms which could be responsible for the line broadening, including static magnetic hyperfine interactions, intermolecular dipolar interactions, and pseudoquadrupole interactions. Currently, a partial decoupling by relaxation seems to us the most plausible explanation of the observed phenomena.

EPR Studies of $[Fe^{III}Cu^{II}(BPMP)Cl_2](BPh_4)_2$. Using a bimodal cavity we have studied the X-band EPR spectra of $[Fe^{III}Cu^{II}$-

(13) Holman, T. R.; Andersen, K. A.; Anderson, O. P.; Hendrich, M. P.; Juarez-Garcia, C.; Münck, E.; Que, L., Jr. *Angew. Chem., Int. Ed. Engl.* **1990**, *29*, 921–923.

(14) As discussed in ref 13, the signs of the coupling interactions for **1** and $[Fe^{III}Cu^{II}BPMP(OAc)_2](BPh_4)_2$ can be understood from a consideration of the relative orientations of the magnetic orbitals on the Fe^{III} and the Cu^{II} ions. The Cu^{II} ion in **1** is square pyramidal with the phenolate at the apex, so the magnetic orbital ($d_{x^2-y^2}$) is orientated perpendicular to the Cu–$O_{phenolate}$ bond. In $[Fe^{III}Cu^{II}BPMP(OAc)_2](BPh_4)_2$, the Cu^{II} ion is six-coordinate with its Jahn–Teller distortion axis perpendicular to the Cu–$O_{phenolate}$ bond; such a geometry places the Cu–$O_{phenolate}$ bond in the plane of the magnetic orbital. If the phenolate oxygen is assumed to be the principal conduit for the magnetic interaction, **1** would be expected to be ferromagnetic since the iron magnetic orbitals are orthogonal to that of the Cu^{II}, while $[Fe^{III}Cu^{II}BPMP(OAc)_2](BPh_4)_2$ would be antiferromagnetic because the magnetic orbitals of the Fe^{III} and the Cu^{II} ion can overlap at the phenolate oxygen.

(15) (a) Spijkerman, J. J.; Hall, L. H.; Lambert, J. L. *J. Am. Chem. Soc.* **1968**, *90*, 2039–2043. (b) Hall, L. H.; Spijkerman, J. J.; Lambert, J. L. *J. Am. Chem. Soc.* **1968**, *90*, 2044–2048. (c) Reiff, W. M.; Long, G. J.; Baker, W. A., Jr. *J. Am. Chem. Soc.* **1968**, *90*, 6347–6351.

(16) Rusnak, F. M. Ph.D. Thesis, University of Minnesota, 1988, Chapter 3, pp 126–127.

(17) Rusnak, F. M.; Münck, E.; Nitsche, C. I.; Zimmermann, B. H.; Fee, J. A. *J. Biol. Chem.* **1987**, *262*, 16328–16332.

(18) (a) Averill, B. A.; Davis, J. C.; Burman, S.; Zirino, T.; Sanders-Loehr, J.; Loehr, T. M.; Sage, J. T.; Debrunner, P. G. *J. Am. Chem. Soc.* **1987**, *109*, 3760–3767. (b) Sage, J. T.; Xia, Y.-M.; Debrunner, P. G.; Keough, D. T.; de Jersey, J.; Zerner, B. *J. Am. Chem. Soc.* **1989**, *111*, 7239–7247. (c) Sage, J. T. Ph.D. Thesis, University of Illinois, 1986.

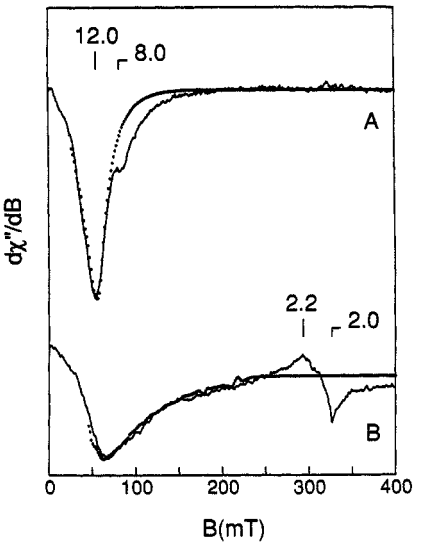

Figure 7. EPR spectra (solid lines) and simulations (dotted lines) of a 0.8 mM acetonitrile solution of $[Fe^{III}Cu^{II}(BPMP)Cl_2](BPh_4)_2$, using a microwave field $\mathbf{H}_1$ parallel (A) and perpendicular (B) to the static magnetic field **H**. The simulation parameters used for the $S = 3$ multiplet were $D = 0.65$ cm^{-1} $\sigma_D = 0.15$ cm^{-1}, $E = 0.06$ cm^{-1}, $\sigma_E = 0.02$ cm^{-1}, $\mathbf{g} = 2.00$ (isotropic). Instrumental parameters: temperature, 2.5 K; microwave frequency, 9.1 GHz at 0.02 mW (unsaturated); modulation frequency, 100 kHz at 0.1 mT_{pp}; gain = 4×10^4; $dH/dt = 0.8$ mT/s. The signal near $g = 2$ in part B is from a preparation-dependent Cu^{II} impurity; if treated as an $S = {}^1/_2$ system the impurity has a concentration of 0.06 mM. The theoretical curves for $B < 25$ mT are not shown. As the field approaches $B = 0$, an increasingly finer grid is required for the powder integration, demanding considerably longer computation time.

$(BPMP)Cl_2](BPh_4)_2$ in acetonitrile. Spectra were taken in the temperature range from 2 to 50 K. The concentration of the complex was varied to assure that the signals were not affected by intermolecular magnetic interactions. (EPR spectra of polycrystalline samples show integer spin signals, but they bear little resemblance to the solution spectra.) Spectra recorded at 2 K under nonsaturating conditions in parallel mode (microwave magnetic field $\mathbf{H}_1$ parallel to **H**) and perpendicular mode are shown in Figure 7. Resonances are observed at $g = 12$, 8, and 2 ($g = h\nu/\beta H$). The signal around $g = 2$ is most likely due to a copper impurity; this signal is preparation dependent and is suppressed in parallel mode.

The $g = 12$ resonance exhibits increased intensity in parallel mode. This observation taken together with the position and line shape of the signal is characteristic of a system with integer electronic spin.[6] Such resonances arise from transitions between levels of a quasidegenerate doublet (splitting $\Delta < 0.3$ cm^{-1}), for which the resonance condition can be written as

$$(h\nu)^2 = \Delta^2 + (\tilde{g}\beta H)^2 \qquad (8)$$

Here $\tilde{g} = g_{eff} \cos \alpha$, where α is the angle between the static field H and an appropriate molecular axis, and g_{eff} is the effective g value of the doublet. The intensity of the $g = 12$ resonance is approximately inversely proportional to temperature as the temperature is lowered to 2 K, showing that it originates from a ground doublet.

The interpretation of the $g = 12$ signal can be addressed with methods described recently by Hendrich and Debrunner[6] and by Hendrich et al.[1] Application of these methods provides strong arguments that the resonance belongs to a multiplet with $S = 3$. However, since the spin of complex **1** has been determined from the 5.0 T Mössbauer spectra of Figure 4, we will proceed with analysis of the signal using eq 2. It will be useful to designate the states of the $S = 3$ multiplet with labels appropriate for $|D| \gg \beta H$ and small E/D values, $|3,m^{\pm}\rangle = (|3,+m\rangle \pm |3,-m\rangle)/\sqrt{2}$.

The $g = 12$ signal can be assigned to transitions between the $|3,3^{\pm}\rangle$ levels if $D < 0$ or to transitions between the $|3,0\rangle$ and $|3,1^{-}\rangle$ levels if $D > 0$. As discussed in the preceding section the former case can be eliminated by the Mössbauer data. Therefore, we focus here on the doublet $|3,0\rangle$, $|3,1^{-}\rangle$ noted in Figure 2B. This doublet has an easy axis of magnetization along y,[19] i.e. the Zeeman splitting is large when the applied field is directed along y and small when the field is along x or z.

The parameters of Table I and use of eq 1 give for the splitting of the doublet $\Delta = 0.36$ cm^{-1}. This value is slightly too large to fit the inequality $h\nu < 0.3$ cm^{-1} for X-band spectroscopy. However, it should be noted that the 0.5 T Mössbauer spectrum suggests that the zero-field splitting parameters are distributed. This is also evident from consideration of the line width of the $g = 12$ resonance. The observed width, approximately 40 mT in parallel mode, cannot be explained solely by unresolved magnetic hyperfine interactions (see below) or by the intrinsic spin-packet width.[6] If D and E are distributed, the splitting Δ is distributed as well, and thus a substantial fraction of molecules (our simulations indicate about 50%) will have Δ values that are smaller than 0.3 cm^{-1}. These molecules are observed with X-band EPR.

In order to analyze intensity and line shape of the $g = 12$ resonance we have developed a computer program that diagonalizes eq 2 and computes the EPR intensities for parallel and transverse mode spectra. The program was created by modifying routines previously used to simulate spectra of $S = 2$[6,20] and $S = 4$[1] systems. We have recently fitted successfully the spectra of some $S = 2$ and 4 systems by assuming that D is sharp and that E has a Gaussian distribution. For complex **1**, however, all attempts to fit the line shape with a fixed value for D were unsuccessful, and we thus felt compelled to use a distribution for D as well. The necessity of including a distribution in D is not surprising given that the EPR spectrum is critically dependent on $\Delta = \Delta(E,D)$ and that $(d\Delta/dE)/(d\Delta/dD) \approx 4$ at $E/D = 0.09$. The results of our spectral simulations of the $g = 12$ resonance are shown in Figure 7; the zero-field splitting parameters used and distribution widths were $D = 0.65$ cm^{-1}, $\sigma_D = 0.15$ cm^{-1}, $E = 0.06$ cm^{-1}, and $\sigma_E = 0.02$ cm^{-1}.[21] The same parameter set predicts both the parallel and perpendicular line shape without use of an additional parameter. Moreover, with reference to a standard sample, this parameter set predicts the absolute intensity of the spectra of Figure 7.[22]

Both Mössbauer and EPR spectroscopy give the same value for E/D, and the D values agree within the uncertainties. Since the $g = 12$ resonance belongs to a doublet with an easy axis of magnetization along y, EPR is sensitive only to the y component of the **g** tensor of eq 2. We found that $g_y = 2.0$ gives satisfactory fits to the data. Equation 4 shows that the $S = 3$ state is not very sensitive to the **g** anisotropy of the Cu^{II} site because $\mathbf{g}_z$ is scaled down by the factor 1/6. We have synthesized a $Ga^{III}Cu^{II}$ analogue of complex **1**, namely $[Ga^{III}Cu^{II}(BPMP)Cl_2](BPh_4)_2$ where the

(19) In zero magnetic field and for $E/D = 0.09$ the two lowest levels of complex **1** are approximately $|3,0\rangle$ and $|3,1^{-}\rangle = (|3,+1\rangle - |3,-1\rangle)/2^{1/2}$. Under conditions where mixing with higher levels by the Zeeman term is negligible, the only nonvanishing Zeeman matrix element between the two lowest levels is $\langle 3,1^{-}|g_y\beta S_y H_y|3,0\rangle = -i(6^{1/2})g_y\beta H_y$. Consequently, the Zeeman interaction is uniaxial, with an easy axis along y. The present approximation yields $g_{eff} = 24^{1/2}g_y = 9.8$ for $g_y = 2.0$ while the exact treatment with diagonalization of eq 2 yields $g_{eff} = 10.8$.

(20) Hendrich, M. P.; Debrunner, P. G. *J. Magn. Reson.* **1988**, *78*, 133–141.

(21) The value quoted for D was not directly obtained from the EPR simulations. With use of eq 2 for $S = 3$ the simulations gave for the splitting of the ground state the value $\Delta = 0.32$ cm^{-1}. For $E/D = 0.09$ the spin Hamiltonian of eq 2 yields $\Delta = 0.55$ D. However, as pointed out above, for small values of J the $S = 3$ and 2 multiplets mix, and Δ becomes dependent on J. For $J = -3$ cm^{-1} and $D_1 = 1.2$ cm^{-1} the mixing decreases Δ by 23%. Thus, $D = (2/3)D_1$ will be about 23% smaller when it is analyzed without taking mixing into account. While we have programs that simulate Mössbauer spectra using either the coupled or uncoupled representations, we do not yet have a program that simulates the EPR spectra from eq 1; we have therefore adjusted the value of D obtained from eq 2 by 23%.

(22) The simulated intensity of the perpendicular mode spectrum appears to be 20% higher than that of the data. This intensity depends on an accurate determination of both the strength of the microwave field and the filling factor for the perpendicular microwave mode relative to the parallel mode. These quantities are typically determined with a ±10% uncertainty. While the 20% mismatch is close to acceptable, we have obtained better agreement in previous work.[1,6] To obtain a better match to the amplitude we have reduced the intensity of the simulated spectrum of Figure 7B by 20%.

diamagnetic Ga^{III} replaces the paramagnetic Fe^{III}. In acetonitrile the complex exhibits $g_{\parallel} = 2.28$ and $g_{\perp} = 2.03$ for the Cu^{II} site. Thus, only if $g_{\parallel}(Cu^{II})$ would correspond to the y direction of complex **1**, would one expect an appreciable deviation from $g = 2.0$, namely $g_y = 2.05$. The $g = 12$ resonance, however, is too broad to determine such deviations.

The EPR spectra of Figure 7 show a weak resonance at $\mathbf{g} = 8$ which, according to its temperature dependence, originates from excited states. Inspection of the energy levels of the coupled system for $E/D = 0.09$ reveals that three excited state doublets could contribute to this resonance. Possible transitions at $\mathbf{g} = 8$ would involve the $|3,2^+\rangle \Leftrightarrow |3,2^-\rangle$ pair of the $S = 3$ multiplet and the $|2,0\rangle \Leftrightarrow |2,1^-\rangle$ and $|2,2^+\rangle \Leftrightarrow |2,2^-\rangle$ pairs of the $S = 2$ manifold. The transition probabilities of the $|3,2^+\rangle \Leftrightarrow |3,2^-\rangle$ and $|2,2^+\rangle \Leftrightarrow |2,2^-\rangle$ pairs are more than an order of magnitude smaller than that of the ground-state resonance. The levels $|2,0\rangle \Leftrightarrow |2,1^-\rangle$, for the given D_1 and E_1, have an average $\Delta > 0.3$ cm^{-1} and thus most molecules do not fall into the energy window of X-band spectroscopy (see Figure 8, below). These factors, coupled with the smaller populations of the states, rationalize the observed weakness of the $g = 8$ resonance. Moreover, we have observed that width and intensity of the $g = 8$ signal changes in a freeze–thaw cycle. For these reasons we have excluded the $g = 8$ resonance from our spectral simulations.[23]

Determination of the Spin Concentration. EPR is predominantly applied to compounds with half-integral electronic spin. For solids or frozen solutions one typically obtains g values, information about zero-field splittings, exchange parameters, and hyperfine parameters. For biological applications much effort has additionally been directed toward the determination of the spin concentration. For Kramers systems, this procedure involves integration of the EPR spectrum and comparison with a suitable standard. For systems where signals are only observed below 20 K, spin quantitations typically have uncertainties of ±10%. The uncertaintly is largely due to difficulties in obtaining accurate temperature measurements in the helium gas flow systems widely used. For systems with integer spin such as Fe^{II} compounds or the cluster described here, only a few attempts in determining the spin concentration have been reported.[1,4c,6]

Complex **1** exhibits an EPR signal for which good simulations are now available and the relevant electronic properties of the cluster are now well understood by the combined EPR and Mössbauer study. Therefore, it is possible to determine the spin concentration of complex **1** directly from the EPR spectra of Figure 7. For this determination, the acetonitrile solution of the Mössbauer sample was transferred into an EPR tube. The sample gave the spectra of Figure 7. Immediately after recording these spectra, the spectrum from a single crystal of Fe^{II} doped into zinc fluorosilicate was recorded for use as the standard.[24] The spectra of both complex **1** and the standard were then simulated and compared. This procedure yielded an $S = 3$ spin concentration of 0.8 ± 0.25 mM. We have used only the $g = 12$ resonance in parallel mode for determining the spin concentration. If the $g = 8$ signals are indeed excited states of complex **1**, our spectral simulations make proper allowance for the population of excited states by specifying D, E, and the temperature of measurement. After completing the measurements an aliquot was removed from the EPR sample, and a cluster concentration of 0.8 ± 0.1 mM was determined optically, using $\epsilon = 1400$ M^{-1} cm^{-1} at 604 nm. The Mössbauer data show that all iron of the sample belongs to complex **1**. Moreover, the electronic parameters obtained by EPR and Mössbauer spectroscopy agree, showing that the $g = 12$ resonance results from the species which accounts for all the Mössbauer absorption. The copper impurity visible by EPR is not expected to contribute more than about 1% to the extinction at 604 nm.[25] With this information, the spin concentration determined by analysis of the $g = 12$ signal and the optically determined cluster concentration are in excellent agreement.

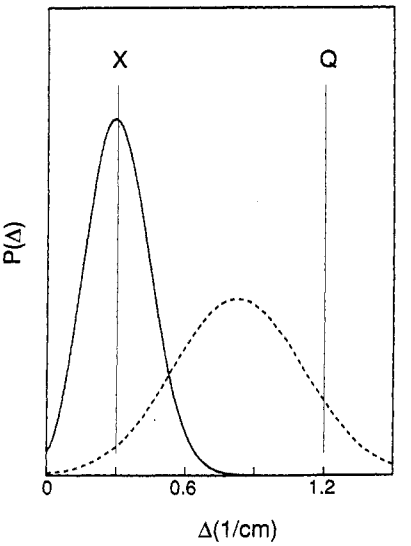

Figure 8. Probability distributions for the spitting Δ of the ground doublet (solid line) and the lowest doublet of the $S = 2$ manifold (dashed) of complex **1**. The plots were generated from the simulation parameters given in Figure 7. The vertical lines at 0.3 and 1.2 cm^{-1} indicate the resonance energies for X- and Q-band microwave frequencies, respectively. Only those molecules having Δ values to the left of the vertical lines will show resonances for the chosen microwave energy.

Conclusion

We have studied here an exchange-coupled $Fe^{III}Cu^{II}$ complex with integer electronic spin that yields well-resolved Mössbauer spectra and a strong EPR resonance at X-band. A very attractive attribute of complex **1** is that it not only allows observation of a well-defined EPR resonance but the cluster contains a high-spin ferric site for which the hyperfine interactions are readily analyzed, primarily because the magnetic hyperfine interaction is isotropic; the spectrum of Figure 4A demands that A is isotropic to better than ±1%. Thus, complex **1** is ideally suited to study the feasibility of quantitative EPR of an integer spin system with sizable zero-field splittings. We do not know of any mononuclear integer spin system (e.g. high-spin Fe^{II}) for which one could carry out such a combined Mössbauer and EPR study with similar accuracy.

We have recently published a quantitative analysis of the EPR spectra of the $Fe^{II}Fe^{II}$ cluster of reduced methane monooxygenase.[1] The two high-spin ferrous sites of this cluster are ferromagnetically coupled, and the cluster yields an integer-spin resonance. For testing the feasibility of quantitative EPR, reduced methane monooxygenase has two disadvantages. First, the Mössbauer spectra of its two ferrous sites are ill resolved and currently not understood. Second, while the Fe concentration of methane monooxygenase samples can be determined accurately, the fraction of iron belonging to the ferromagnetic cluster was not known. On the other hand, the desire for understanding this catalytically

(23) During the past year we have studied 8 different preparations of complex **1** in acetonitrile. Six samples gave EPR spectra essentially identical with those reported here. Two samples showed a resonance that was somewhat broadened and shifted from $g = 12$ to 13.2. The spectra could not be interconverted by freeze–thaw cycling. The 1.0 and 6.0 T Mössbauer spectra of two samples exhibiting the different signals were virtually identical. The differences between samples exhibiting a $g = 12$ or 13.2 resonance can be explained by assuming that the latter have a D value which is 0.1 cm^{-1} larger than that of the former.

(24) A polycrystalline sample of iron-doped zinc fluorosilicate would simplify the calculations as no filling factor correction is then needed. However, for as yet undetermined reasons, EPR signals from crushed crystals are not always reproducible.

(25) The impurity signal around $g = 2$ is only observed in the transverse mode, suggesting that it belongs to a Kramers system such as Cu^{II} or a weakly coupled ($J \ll \beta H$ at 0.3 T) $Cu^{II}Cu^{II}$ pair. We have observed this species in variable amounts in different preparations. Treated as a spin = $^1/_2$ system, the $g = 2$ signal of Figure 7B has a spin concentration of 0.06 mM, i.e. less than 8% of that of the $g = 12$ species. We have observed that the Cu/Fe ratio of some of the preparations is slightly larger than 1. It is unlikely that the $g = 2$ impurity contributes significantly to the optical spectrum at 604 nm; per Cu the extinction coefficients of $[Ga^{III}Cu^{II}(BPMP)Cl_2](BPh_4)_2$ and $[Cu^{II}Cu^{II}(BPMP)Cl_2](BPh_4)_2$ at 604 nm are less than 5% of that of complex **1** (unpublished results).

competent state of methane monooxygenase has been a driving force for developing the quantitative aspects of integer-spin EPR. The results obtained here indicate that EPR of integer-spin systems can be used to determine spin and zero-field splitting parameters and to provide an accurate determination of spin concentrations.

The EPR spectra reported here are typical of those observed for integer-spin complexes with large zero-field splittings. Spectra obtained in frozen solution exhibit rather broad features with line shapes dominated by distributions of zero-field parameters. The splitting of the EPR active doublet $\Delta(D,E)$ is also spread and the spread tends to straddle the X-band microwave energy. The resonance condition, eq 8, can only be satisfied for $\Delta < h\nu \approx 0.3$ cm^{-1}, thus, only a fraction of the molecular distribution is observed. Consequently, the success of spin quantitation depends on our ability to find the correct distributions for D and E, to allow a prediction of the fraction of molecules with $\Delta < h\nu$. The work described here shows that the spin concentration can be determined with good accuracy. While we are confident that such quantitation can be obtained for many other systems, we consider it advisable to study more systems where the results can be checked with a powerful technique such as Mössbauer spectroscopy. With more experience, it should be possible to venture with more confidence to systems such as Ni^{II} or Mn^{III} where EPR may have to stand on its own.

Substantial information of the spin system in question can be added by extending measurements to multifrequency EPR.[4a] Studies at additional frequencies not only give a cross-check of the parameters obtained at X-band, but in many cases it may be possible to observe additional resonances from a different pair of levels or from a species that is EPR silent at X-band. As an example consider complex **1**. Figure 8 shows a plot of the probability distribution of Δ values for the $|3,0\rangle$, $|3,1^-\rangle$ pair (solid line) computed from the distributions of D and E used for the simulations of Figure 7. The vertical line at 0.3 cm^{-1} corresponds to the X-band microwave energy, i.e. only molecules with $\Delta <$ 0.3 cm^{-1} (left of line) contribute to the $g = 12$ resonance; the fraction is ≈50%. On the other hand, at Q-band (vertical line at 1.2 cm^{-1}) all molecules of the sample would be EPR active. Now consider the lowest pair of levels from the excited $S = 2$ quintet (see Figure 2) of complex **1**. The probability distribution of Δ values for the $|2,0\rangle$, $|2,1^-\rangle$ pair ($g_{eff} \approx 8$) is shown in Figure 8 (dashed line) as computed from the same parameter set. As mentioned above, only a small fraction of molecules is observed at X-band, whereas Q-band spectroscopy would show signals from virtually the entire molecular population.

Acknowledgment. We thank Prof. Oren Anderson and Kevin Andersen for their generous help in solving the structure of the FeCu complex. We are grateful to Prof. J. D. Lipscomb for allowing us frequent use of his EPR instrument. This work was supported by the National Institute of Health through Grants GM-38767 (L.Q.) and GM-22701 (E.M.), predoctoral traineeship GM-08277 (T.R.H.), and postdoctoral fellowship GM-12996 (M.P.H.).

Models of Lysine–Cysteine Hydrogen Bonding in Metallothionein: Hydrogen Bonding between Ammonium and Benzenethiolate in $[(C_6H_{11})_2NH_2]_2[Co(SC_6H_5)_4]$

Wesley P. Chung, John C. Dewan, and M. Anton Walters*

Contribution from the Department of Chemistry, New York University, New York, New York 10003. *Received May 7, 1990*

Abstract: Anion–cation hydrogen bonding interactions are described for $[(C_6H_{11})_2NH_2]_2[M(SC_6H_5)_4]$ where M = Co (**1**), Zn (**3**), which serve as models of putative lysine–cyteine hydrogen bonding at the metal binding site of metallothionein. Complex **1** is isolated as green crystals in which an average N–H···S hydrogen bond length of 3.29 (1) Å is observed in infinite one-dimensional chains. The dicyclohexylammonium counterion occupies a bridging position by hydrogen bonding to thiolate ligand sulfur atoms on adjacent anion complexes. There are two $[Co(SC_6H_5)_4]^{2-}$ anions per asymmetric unit where each Co atom is tetrahedrally coordinated by four benzenethiolate ligands [Co–S_{av} = 2.308 (4) Å]. In the non-hydrogen bonding complex $[(CH_3)_4N]_2[Co(SC_6H_5)_4]$ (**5**), a split vibrational band at 228 cm^{-1} (av) is assigned to a Co–S T_2 related mode. In $[(CH_3)_4N]_2[Zn(SC_6H_5)_4]$ (**7**) this band is replaced by one at 199 cm^{-1}. Relatively intense bands at 192 and 180 cm^{-1} in the Raman spectra of **1** and **3** are assigned to metal–ligand modes. Hydrogen bonding causes a decrease in metal–ligand bond length of 0.02 Å relative to the bonds in a non-hydrogen bonding complex.

Introduction

In the Zn- or Cd-containing forms of metallothionein (MT) metal ions are coordinated exclusively by cysteine (Cys) ligands in two binding sites M_4–Cys_{11}^{3-} and M_3–Cys_9^{3-}, designated α and β.[1] The coordination geometry of each metal ion is approximately tetrahedral.[1] There are seven positions along the polypeptide chain of MT where Cys and lysine (Lys) are adjacent. This has been considered to be of possible importance in the structure and stability of the metal binding sites of the protein. Vasak and co-workers[2,3] reported an unusually high pK_a for the Lys side chains. Demetalation of the protein in acidic solution caused a decrease in the Lys pK_a from 10.9 to 10.3. The deprotonation of Lys caused changes in the circular dichroism spectrum of the protein which were attributed to electrostatically induced structural alterations. In addition, the arylation of Lys by trinitrobenzenesulfonic acid resulted in changes in the CD spectrum of Cd–MT. The metal-free *S*-carboxamidomethyl derivative of MT had an average pK_a of 10.3 which differs from the value of 10.9 measured in the native protein. Taken together, these effects were argued to be consistent with the interruption of hydrogen bonds between Cys and Lys. It was suggested that hydrogen bonding to the cationic Lys side chain might serve to stabilize the met-

(1) Furey, W. F.; Robbins, A. H.; Clancy, L. L.; Winge, D. R.; Wang, B. C.; Stout, C. D. *Science (Washington, D.C.)* **1986**, *231*, 704–710.
(2) Vasak, M.; McClelland, Ch. E.; Hill, H. A. O.; Kagi, J. H. R. *Experientia* **1985**, *41*, 30–34.
(3) Pande, J.; Vasak, M.; Kagi, J. H. R. *Biochemistry* **1985**, *24*, 6717–6722.

0002-7863/91/1513-525$02.50/0